

УДК 532.771

*Ladislav Lazić – Prof., dr. sc., Faculty of Metallurgy, University of Zagreb, Sisak, Croatia*

*Augustin Varga – Prof., CSc., Faculty of Metallurgy, Technical University, Košice, Slovakia*

*Vladimir L. Brovkin – Doc., CSc, Department of Heat Engineering and Ecology, National Metallurgical Academy of Ukraine, Dnepropetrovsk, Ukraine*

*Jan Kizek – Doc. Ing., CSc., Faculty of Metallurgy, Technical University, Košice, Slovakia*

## **INFLUENCE ANALYSIS OF THE STRUCTURAL DEFECTS IN THE CASTING LOAD ON THE HEATING RATE**

*The object of this paper was to examine the structural defects that influence the mechanical properties of circular cross-section continuous steel casting (API N80) intended for the rolling mill production of the seamless tubes. The values of ultimate strength for tensile specimens at different temperatures are obtained from the standard tensile test. Optical and Scanning Electron Microscope (SEM) are used in investigations of the microstructural features of material structure and defects. The mathematical model of heating process of steel load in the rotary-hearth furnace, which enables the required thermal analysis, was constructed on the basis of the finite element method (FEM). Transient heat conduction and thermal stress analysis were performed in order to determine the heating rate and, via the temperature variation throughout the structure, thermal stresses and deformations.*

### **INTRODUCTION**

Valjaonica cijevi Sisak (today's firm is Commercial Metals Company d.o.o., Sisak) produces seamless tubes for the Oil Tubular Goods, Line Pipes and Drill Pipes, under API standards, by the route Electric Arc Furnace-Ladle Furnace-Continuous Casting Machine- Rotary-Hearth Furnace-Rolling Mill. Al- and Si- deoxidation, alloying and degassing are carried out in the ladle furnace. The continuous casting of the killed types of steel is performed in the vertical continuous casting plant. The continuous casting steel semi products serve as the load, being heated in the rotary-hearth furnace before hot rolling into seamless tubes.

In the present investigation, the cast furnace load of circular cross-section of 410 mm and length of 1500 mm was researched. Steel grade of

the load is N80, according to the API standard. The composition of the steel is given in Table 1.

Table 1

*Chemical composition of steel N80*

Element	C	Mn	Si	Al	V	Al	P <sub>max</sub>
%	0,30- 0,34	1,15- 1,30	0,15 – 0,35	0,02 – 0,04	0,15 – 0,18	0,02- 0,04	0,025

Element	S <sub>max</sub>	Cu <sub>max</sub>	Sn <sub>max</sub>	Cr	Ni	Mo	(Cu+8Sn) <sub>max</sub>
%	0,025	0,25	0,03	0,15	0,18	0,02	0,45

In the rolling mill production of the seamless tubes, the faults of final products may appear due to the cracks caused by the thermal stresses at the beginning of heating process in the rotary-hearth furnace while the load is not plastic enough, i.e. in the temperature range under 500 °C [1,2,3].

Since the mechanical properties are influenced by the presence of inclusions in steel, the objective of this paper is to establish the size and distribution of non-metallic inclusions (NMI) and pores across the cross-section of the continuous casting load as well as their impact on the tensile strength. The obtained results will serve in the subsequent thermal stress analysis, questioning whether the temperature differences, appearing through the cross-section of the load heated in the rotary-hearth furnace, lead to the thermal stresses which exceed the tensile strength of the load and cause the stress cracks in the load structure.

The investigation methodology consists of the next phases:

- Testing the tensile strength of the specimens taken on the different places of cross-section of the cut cast furnace load;
- Examinations of the microstructural features of material structure and defects on the tested tensile specimens using Optical and Scanning Electron Microscope;
- Measurements of the controlled parameters of temperature regime during heating of the steel load;
- Formulation of the mathematical model on the basis of the finite element method;
- Transient heat conduction analysis through the model simulations in order to determine the temperature distribution throughout the structure and the heating rate;
- Thermal stress analysis in order to determine the thermal stresses and deformations.

## TENSILE TEST

This study used a standard tensile specimen with a circular cross-section to conduct tensile stress–strain tests. The specimens were taken from the mid-thickness location of the cut load and came in two series all over the cross-section, starting from the surface, across the core to the opposite end. In this sequence, the specimens were tested at the test temperatures from 100 up to 650 °C, with the step of 50 °C.

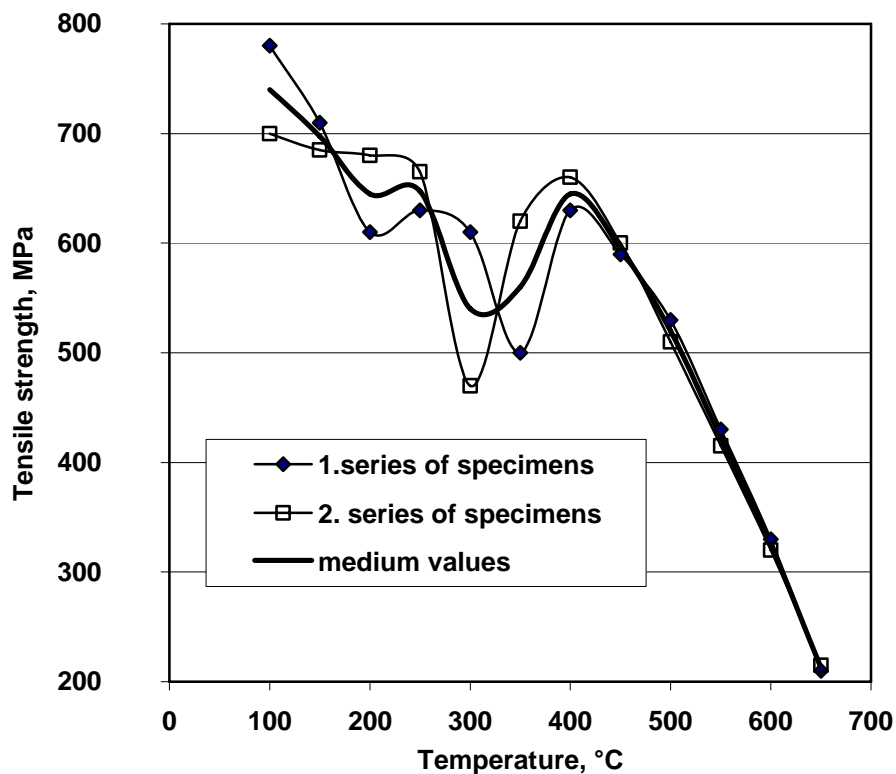


*Figure 1. The distribution of tensile properties versus the test temperature*

The distribution of tensile properties versus the test temperature in the form of diagram is shown in Fig. 1. It may be seen that, at the specimen cut from the core of the casting, the tensile strength is for 190 MPa lower in comparison to the specimen taken from the surface zone. Accordingly, the tensile strength of the core is lower in relation to the surface zone of the casting for 25 – 30 %. The cause of this phenomenon may only be the metallurgical cleanness of the casting.

## MICROSTRUCTURE ANALYSIS

As a general rule, the solidification grain structure of the cross-section of continuous casting consists of an outer *chill* (or outer equiaxed) zone comprising fine, randomly-oriented grains, an *intermediate columnar zone* comprising elongated, oriented grains and a *central equiaxed zone*, again comprising randomly-oriented grains [4]. One or another of these zones may be small or absent in any given casting. The interrelation of these zones depends on a few factors such as: steel composition, shape and size of casting cross-section, temperature and rate of casting, intensity of primary and secondary cooling.

The structure, distribution of segregations and non-metallic inclusions, as well as other qualitative characteristics, differ widely between individual cross-sections because the shape and size of the cross-section of continuous castings influence the crystallization process. The manner of final meetings of the crystallization fronts depends on the shape of the casting (mould) cross-section. At the circular or square cross-section the crystallization fronts meet in the one point and at rectangle cross-section in the one line. The latter is more favourable in view of the distribution of non-metallic inclusions and segregations.

On the cross-section macrostructure of the cut casting it might be seen the cracks between the outer chill and intermediate columnar zone, the cracks extending in the intermediate columnar zone in the direction of solidification and the porosity and inclusions in the central equiaxed zone.

Regarding microinclusion cleanliness rating, it was evaluated in the observed casting product by the means of light microscope based methods, which consider the shape, size and amount of microinclusions such as sulfides, oxides, silicates etc. From the specimens subjected to the tensile test, one from the outer zone (very close to the surface) and other from the core, the specimens for microstructure analysis were prepared.

The optical micrographs of the specimens at the surface of the casting shows the oxide inclusions of very small sizes distributed uniformly all over the cross-section. There is no important porosity. In the case of the specimen from the core (Fig. 2), many pores on the central part of the image (large dark

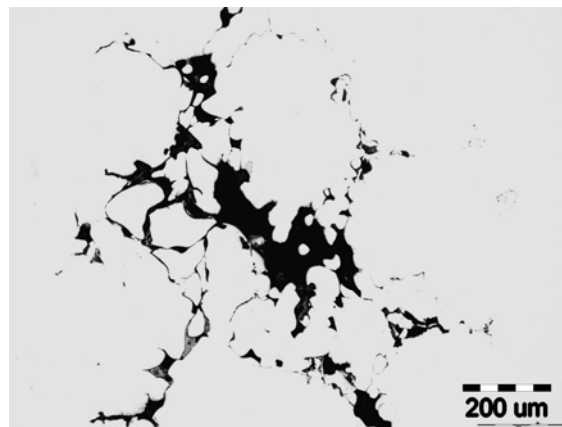
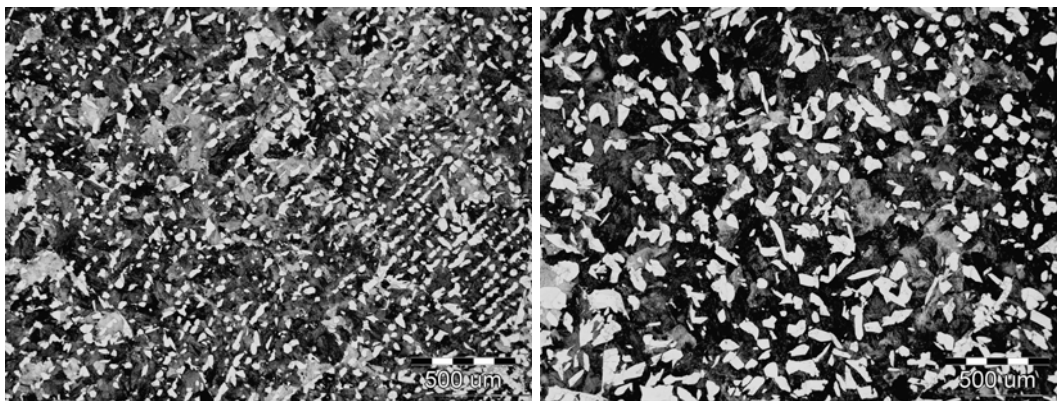


Figure 2. Optical micrograph of the specimen

regions) may be seen. The light layer is the metal matrix and the grey supplements are the non-metallic inclusions.

In order to remove the flowed layer produced by polishing and reveal the structural details, the specimen surfaces were etched by the solution of 5 % nitric acid in alcohol (Nital). Optical micrographs of the etched specimens at the surface and the core of the load are shown in Fig. 3. The photomicrograph (Fig. 3a) of the specimen from the surface zone shows the pearlite-ferrite microstructure consisting of the primary  $\alpha$  ferrite (light layers) within the eutectic structure (large regions in darker tints). The arrangement of the primary  $\alpha$  ferrite grains points to the dendritic microstructure characterised by growth of the trunk, from the left upper corner to the right lower corner of the image, defined by the solidification direction and the parallel branches. The specimen from the core (Fig. 3b) has pearlite-ferrite microstructure comprising randomly-oriented grains, characteristic for the *central equiaxed zone*. The coarse-grain structure resulted from the slow cooling rate at the casting core.



a) Surface

b) Core

Figure 3. Optical micrographs the etched specimens at the surface and the core of the casting, 50x

## MEASUREMENT RESULTS OF THE TEMPERATURE REGIME PARAMETERS

Measurements were conducted in the rotary-hearth furnace fired with natural gas during heating the steel load (API N80) of circular cross-sections of 410 mm and length of 1500 mm.

The controlled parameters (variables) of temperature regime are the wall and the load temperatures. The optic pyrometer Optix Keller PB06 was used for the temperature measurements of the load and the furnace wall surfaces. Figure 4 shows the measured parameters of temperature regime at the usual furnace productivity of 12,4 t/h and the heating time of 7,1 hours.

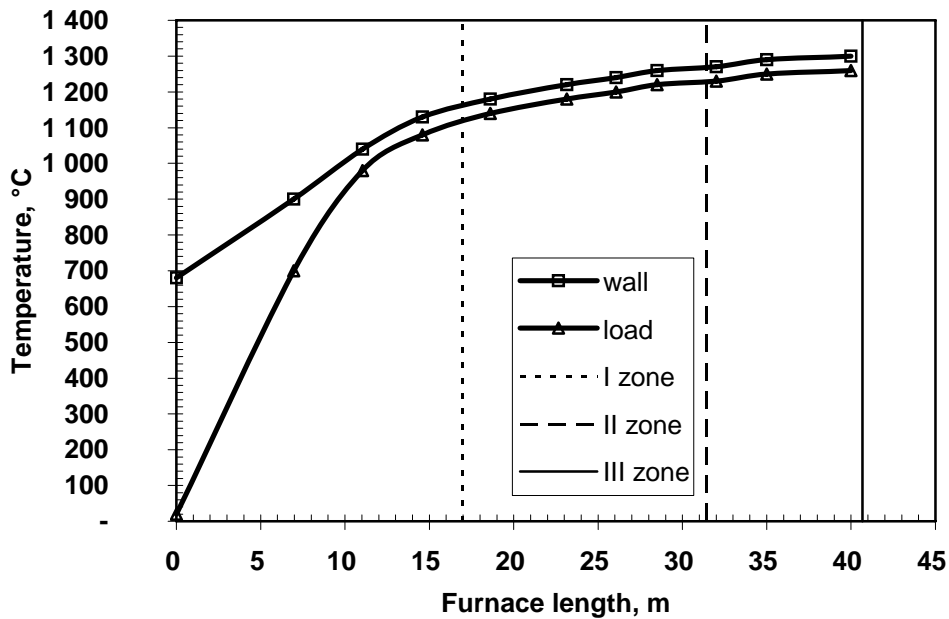


Figure 4. Results of the temperature measurement for the load  $\phi$  410

### FINITE ELEMENT HEATING MODEL

Since the load is very long in relation to the cross section, any cross-section will have the same temperature distribution, i.e. the temperature distribution is constant in the axial direction. Because of the "infinite" length in the Z-direction, it is sufficient to consider only the cross-section in the XY plane. For that reason, the modelling is based on the assumption of a 2-D heat flow. Discretization of the physical problem over a continuous domain into numerous elements is the first step in any analysis. The cross-section under consideration is divided into two-dimensional 4-node quadrilateral elements with the temperature as the only degree of freedom at each node. Since the geometry and the boundary conditions of the cross-section are symmetric in regard to Y-axis, only one half of the cross-section is modelled. Discretization is presented in Figure 5.

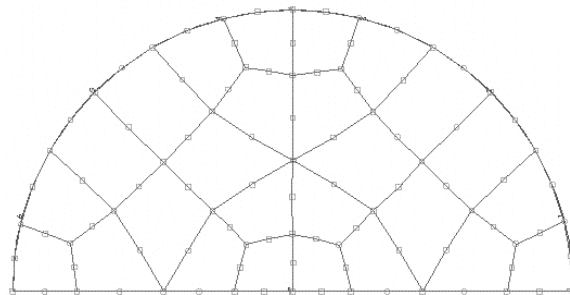


Figure 5. Discretization of the half circular cross-section

*Table 2*  
*The total heat-transfer coefficient,  $h$ , obtained by calculation*

Segment	I	II	III
Distance from the charge door, m	5,66	11,32	16,98
Heating time, h	1,18	1,18	1,18
$h$ , W/(m <sup>2</sup> K)			
- at the beginning	40	105	201
- at the end	110	212	260
- in the middle	67	152	229
Wall temperature, °C			
- at the beginning	680	860	1050
- at the end	860	1050	1160
- in the middle	770	955	1105
Flue gas temperature, °C			
- at the beginning	800	960	1120
- at the end	960	1120	1240
- in the middle	880	1040	1180

The problem under consideration requires convection and radiation boundary conditions for all elements around the closed domain. In thermal analysis, the evaluation of heat exchange coefficients by radiation and forced convection is critical for the reliability of the results. On the basis of temperature measurement results, the temperatures of flue gases and radiation and convective heat transfer coefficients,  $h$ , over the entire length of the single boundary surfaces, were calculated by methodology given in [3, 5, 6, 7]. The values of the total heat-transfer coefficient, temperatures of flue gases and wall temperatures used in the finite element model, are shown in Table 2 for three segments in which the first zone length was divided.

The initial temperature value of the load,  $t = 20$  °C, was specified for the overall structure (nodes) of the cross-section at the beginning of the heating. In this model, all thermal and heat transfer properties were assumed to be directionally independent, as in the "isotropic" material model, i.e. they do not change with any orthogonal transformation of axes. The material properties such as density ( $\rho$ ), specific heat ( $c_p$ ) and thermal conductivity ( $k$ ) are assumed to be temperature dependent.

## **RESULTS OF THE SIMULATION**

Nonlinear transient heat transfer analysis is performed when the material properties and boundary conditions are time dependent and the process involves radiation. These types of problem are solved using an incremental

iterative solution technique. In this case of non-linear transient heat transfer analysis of the circular cross-sections load heating, the modified Newton-Raphson methods (the option of recalculating the conductivity matrix at the beginning of each increment) was used in conjunction with the trapezoidal Crank-Nicholson integration techniques.

The transient heat conduction analysis is performed for furnace production of 12,4 t/h, i.e. for total heating time in the furnace of 7,1 h. In Figure 6, the curves present the model results of temperature variation along the first zone of the load surface, the load centre and the wall surface obtained by the model simulation.

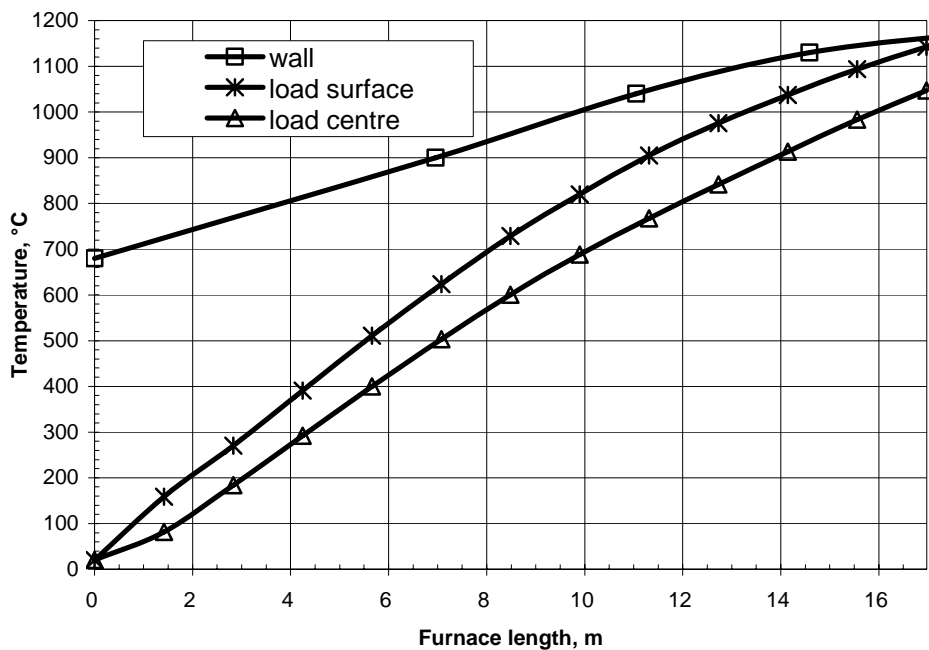


Figure 6. Model results of the first zone heating regime for furnace production of 12,4 t/h

When the body is loaded by the uniaxial stress state, the stress or the strength can be compared directly with *yield strength*, *tensile strength* or *shear strength*. The problem becomes more complicated in the case of bi-axial or triaxial stress state. In those cases, there are a multitude of stresses, but only one significant strength. Whether the body is safe during heating or cooling, a number of *failure theories* have been proposed to answer this question. In this paper, the *maximum-normal-stress theory* was used. According to this theory the failure occurs whenever one of the three principal stresses reaches or exceeds the tensile strength, i.e.

$$\sigma_1 > \sigma_2 > \sigma_3 \quad \sigma_1 \geq R_m,$$

where  $R_m$  is the tensile strength (Pa).



The samples of model results presentation are shown in Figure 7 for the principal stresses and in Figure 8 for the resultant deformations (displacements).

Model results of the load surface temperature, the load centre temperature, the temperature differences between the surface and the centre, as well as principal thermal stresses and resultant deformations are shown in Table 3 for two values of the heating time. Maximal temperature differences through the load cross-section appeared while the load surface temperature varied between 400 and 500 °C.

Table 3

Model results

Distance of the load from the charge door, m	4,24	5,66
Heating time, min	38	50
Temperature of the load surface, °C	391	511
Temperature of the load centre, °C	292	400
Temperature difference, °C	99	111
Principal stress, MPa	169	195
Resultant deformation, mm	2,10	2,96

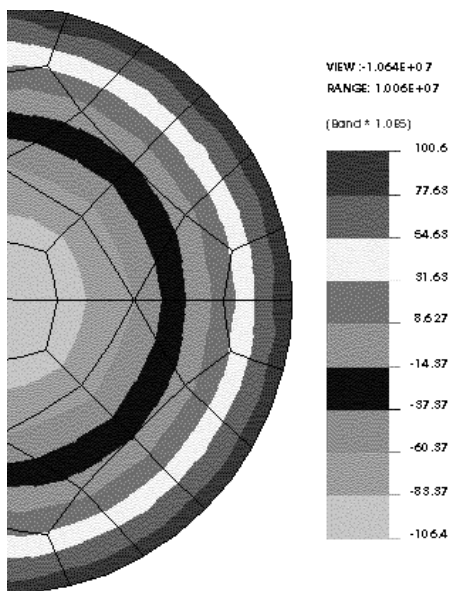


Figure 7. Principal stresses  $\sigma_1$

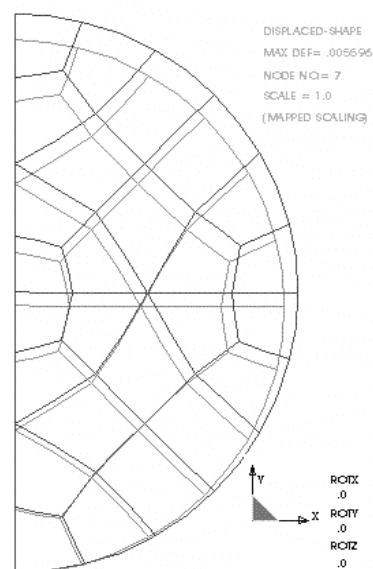


Figure 8. Resultant deformations

## CONCLUSIONS

The experiments in this study suggest that there is a strong correlation between the microstructure and the mechanical properties of the continuous casting. Due to the macrosegregation of the non-metallic inclusions, porosity and the difference in the grain structure, the tensile strength of the core is lower in relation to the surface of the casting for 25 – 30 %.

According to the model results and the measured heating parameters in real conditions, it is established that, at the usual heating rates, the thermal stresses come up to the relative low values, i.e. the temperature difference of about 120°C causes the thermal stresses of about 200 MPa, which is much less in respect to the tensile strength of 530 MPa at 500 °C (Figure 1).

In the case of faster heating at the same temperature regime, the thermal stresses are considerably higher, but still below the values which could cause the appearance of cracks. Merely at the temperature differences of 250 °C, which might only be achieved in some extreme cases, the thermal stresses come up to the values of the tensile strength.

Model is based up to the assumption of the same value of heat transfer coefficient over the entire length of the single boundary surfaces of the cross-section. This assumption was accepted because of simplification of the mathematical model formulation. It is a fact that the unsymmetrical heating only insignificantly increases the temperature differences over the load cross-section, therefore the credibility of the above conclusions is not disputable.

In order to improve the mechanical properties of the furnace cast load and, more importantly, the quality of final rolling products, it is essential to advance the cleanness of the continuous casting products. For a better-grade cleanness control of the continuous casting, the following goals are to be set up [8, 9]:

- To avoid steel reoxidation during the final stage of Ladle Furnace (LF) Process and Continuous Casting;
- To achieve minimum refractory material erosion (tundish lining, shrouds, etc.);
- To avoid ladle and tundish slag vortexing;
- To avoid casting powder (mould liquid slag) entrainment.

## LITERATURE

1. L. Lazić, J. Črnko, *Thermal Analysis During the Cooling of Octagonal Steel Semiproduct*, Acta Mechanica Slovaca 2 (2002) 6, 411 – 416.
2. L. Lazić, J. Črnko, *Finite-Element Thermal Analysis of a New Cooler Design*, Materiali in tehnologije 38 (2004) 3-A, 397 – 402.

3. V. Krivandin, B. Markov, *Metallurgical Furnaces*, Mir Publishers, Moskva, 1980.
4. K. Fisher, *Fundamentals of solidification*, Trans Tech Publications, Aedermannsdorf, Switzerland, 1986.
5. S.B. Vasil'kova et al., *Raschet nagrevatel'nih i termicheskikh pechej*, Metallurgija, Moskva, 1983.
6. W. Heiligenstaedt, *Wärmetechnische Rechnung für Industrieöfen*, Düsseldorf, 1955.
7. J.H. Lienhard IV, J.H. Lienhard V, *A heat transfer textbook*, Phlogiston Press (3rd edition), Cambridge, 2003.
8. R. Tadeusz, P. Krzysztof, Evolution of nonmetallic inclusions and oxygen during production of oxygen converter rail and construction steel, *5<sup>th</sup> Int. conf. on CLEAN STEEL*, Balatonfüred, Hungary, 1997, pp 226 – 235.
9. H. Albasa et al., Cleanliness improvements in oil country tubular goods, *5<sup>th</sup> Int. conf. on CLEAN STEEL*, Balatonfüred, Hungary, 1997, pp. 79 – 88.

*Рукопись поступила 01.04.2008 г.*